Resistance switching at the $Al/SrTiO_{3-x}N_y$ anode interface

A. Shkabko,[1] M. H. Aguirre,[1,a)] I. Marozau,[2] T. Lippert,[2] and A. Weidenkaff[1]
[1]*Solid State Chemistry and Catalysis, Empa, Ueberlandstrasse 129, 8600 Duebendorf, Switzerland*
[2]*Paul Scherrer Institut, 5232 Villigen PSI, Switzerland*

(Received 11 March 2009; accepted 30 April 2009; published online 27 May 2009)

The electroformation and resistance switching behavior of $Al/SrTiO_{3-x}N_y/Al$ have been investigated. The resistance of $Al/SrTiO_{3-x}N_y/Al$ irreversibly increases when voltages higher than a certain threshold voltage are applied. A bistable resistance switching develops at one of the Al electrodes that performs as the anode. The formation of stacking faults in $SrTiO_{3-x}N_y$ during preparation by microwave plasma treatment is a prerequisite for the occurrence of switching as confirmed by site-specific high resolution transmission electron microscopy at the electrode interfaces. The resistance switching effect is discussed by considering the role of stacking fault defects in the oxygen/nitrogen diffusion at the anode metal-oxynitride interface. © *2009 American Institute of Physics*. [DOI: 10.1063/1.3139761]

Binary and ternary transition metal oxides exhibit resistance switching behavior, which comes into operation in resistive random access memory (ReRAM). A bistable switching device as it is used in ReRAM is characterized by two nonvolatile resistance states, a high resistance state (HRS) and a low resistance state (LRS) denoting "0" and "1," respectively. In a typical ReRAM configuration, the transition metal oxide is sandwiched between two metal electrodes representing a metal-oxide-metal (MOM) structure.

In order to obtain a bistable hysteretic current-voltage (*I-V*) behavior, voltages high enough for a resistance change have to be applied.[1] This process is called electroformation and normally stands for the resistance drop by orders of magnitudes.[2] Typically in low-doped ceramic (nearly insulating) materials, the resistance drop is initiated by the voltage-induced dielectric breakdown. The specific feature of dielectric breakdown is the formation of filamentary conducting paths.[3,4] Depending on the sample/electrode size and the electroformation procedure, it can take up to several hours to obtain reliable switching.[5] This reveals slow process of filamentary paths formation and difficulties with their observation by analytical techniques.[6] However, not all the ceramic materials show the resistance drop during electroformation. For example, oxygen deficient $SrTiO_{3-x}$ exhibits nearly Ohmic low resistance prior electroformation. The resistance switches into HRS upon increasing the positive voltage, and returning back to LRS at high negative voltage, yielding the electroformation in a few seconds.[7] The nature of this phenomenon has been explained by the enhancement of oxygen migration due to high electronic current and Joule heat which increase the redox process locally through filamentary paths.[3,7] Based on these results, we suppose that fabrication of ceramics with defined and controlled defect nanostructure would make easy the filamentary path ion conduction prior electroformation. Nevertheless, the relation between the nanostructural defects and the switching behavior has to be understood in more details to produce materials with controllable localization of filaments, fast electroformation, and stable switching.

Strontium titanate is an interesting compound that is highly electronically tunable through doping on cationic/anionic sites. The most studied anionic substitution is O^{2-} by N^{3-}, which is accompanied by the presence of oxygen vacancies and responsible for metallic conductivity similar to $SrTiO_{3-x}$.[8] The nitrogen introduction into $SrTiO_{3-x}$ results in changes of the nanostructure and forms defects. These defects and the amount of N doping can be controlled by plasma treatment parameters such as time and gas flow, as reported previously.[8] In this letter, we investigate the switching behavior and resistance rise during electroformation process in conducting $Al/SrTiO_{3-x}N_y/Al$ by *I-V* measurements and high resolution transmission electron microscopy (HRTEM). The studies are performed directly at the regions of the electrode interfaces to show relationships between the $SrTiO_{3-x}N_y$ (STON) nanostructure and resistance switching properties.

$SrTiO_3$ (100) single crystals grown by the Verneuil method from CRYSTEC with a size of $1\times10\times0.5$ mm^3 were treated in a microwave induced ammonia plasma. Two types of samples were prepared depending on the gas flow rates. The STON-*a* samples were prepared with 125 ml/min and STON-*b* samples with 200 ml/min, as described in detail elsewhere.[9] The composition of the samples on the top surface (0–5 nm) was determined by x-ray photoelectron spectroscopy (XPS) using a PHI Quantum 2000. For electrical conductivity measurements, five microcontacts of Al (25 μm) wires, separated by 1 mm distance, were bonded on the surface by an ultrasound wire bonder (Delvotek 4250). TEM lamellas of the $Al/SrTiO_{3-x}N_y$ interfaces were prepared by focused ion beam (FIB) (FEI Strata 235) to analyze the material before the electroformation process. TEM analysis of the interfaces was performed in a Philips CM30 microscope. The *I-V* measurements were done by the two-probe as well as four-probe method[10] using a dc current source (Keithley 2602) operated in voltage mode with steps of 100 μV/100 μs and a compliance current of 80 mA.

The compositions of both samples were similar within the error of the XPS measurement (~15 at. %), i.e., $\sim Sr_{0.92}TiO_{2.44}N_{0.40}$ for STON-*a* and $\sim Sr_{0.85}TiO_{2.42}N_{0.38}$ for STON-*b*, confirming the N incorporation and Sr deficiency. As it was reported for oxynitrides, the Ti ions are present in Ti^{4+} and Ti^{3+} chemical states accounting for the presence of free electrons and the metallic conductivity in the material (Fig. 1 of supplementary information).[11–15] The chemical

a)Electronic mail: myriam.aguirre@empa.ch.

Author complimentary copy. Redistribution subject to AIP license or copyright, see http://apl.aip.org/apl/copyright.jsp

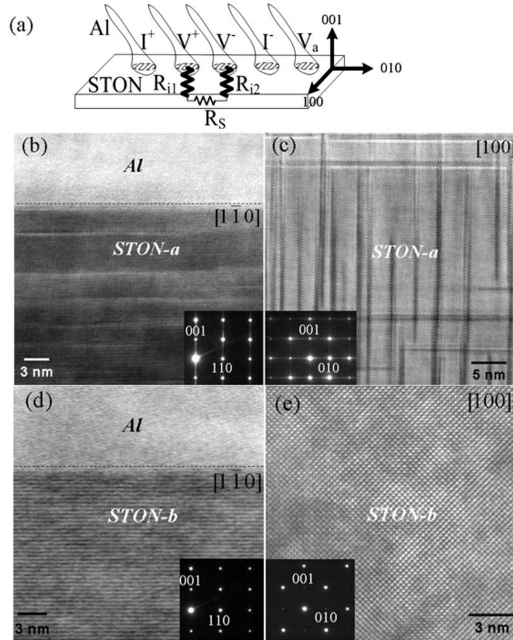

FIG. 1. (a) Diagram of the Al-contact arrangement on the STON surface. (b) HRTEM picture of the Al/STON-*a* interface in [1$\bar{1}$0] orientation. (c) HR-TEM of STON-*a* sample in [100] orientation. (d) HRTEM picture of the Al/STON-*b* interface in the [1$\bar{1}$0] zone axis, (e) HRTEM in [100] orientation. The electron diffraction of each zone axis is inset in the micrographs.

states of O and Sr are not modified with respect to those reported for STO.[12,14,16] Nitrogen ions are incorporated in the STO structure in the oxygen positions and also interstitially. The rate between substitutional and interstitial nitrogen composition is estimated to be 6:1.[8]

Figure 1(a) shows a diagram of the Al-contact arrangement on the $SrTiO_{3-x}N_y$ surface where the voltage and current measurement contacts, i.e., anode and cathode, were prepared. Figures 1(b) and 1(c) show the TEM micrograph of the STON-*a* FIB lamella. Figure 1(b) shows the interface between the Al contact and the STON-*a* in the zone axis [1$\bar{1}$0] of the perovskite structure. The sample reveals stacking faults parallel to the interface. The study on another zone axis, i.e., [100], Fig. 1(c), shows the presence of the defects not only parallel to the surface but also perpendicular to it. The electron diffraction patterns, inset in Figs. 1(b) and 1(c), also corroborates the existence of defects showing the streaking along the directions ⟨001⟩ and ⟨010⟩. This diffuse scattering in the marked directions appears when there are faults in the stacking sequence of the atomic planes.

HRTEM analysis of the same zone axis in sample STON-*b*, displayed in Figs. 1(d) and 1(e) did not show stacking fault defects found before for STON-*a*. These analyses correspond to samples treated at high ammonia flow rates (200 ml/min). However, we cannot exclude the presence of point defects (interstitial nitrogen, oxygen vacancies, Schottky-type defect, Frenkel-type defect, or other electrically active defects) because of a typical black and white contrast representing strains in the STON-*b*. The different defect microstructure on the sample surface plays an important role on the resistance switching properties as discussed in detail below.

The *I-V* curves and electroformation of Al/STON-*a*/Al are measured between V^+ and V^- by the two-point method, as indicated in Fig. 1(a). The total resistance is defined as $R_{total}=R_s+R_{i1}+R_{i2}$, where R_s is the STON-*a* resistance and R_{i1} and R_{i2} are the respective resistances at the Al/STON-*a* interfaces.

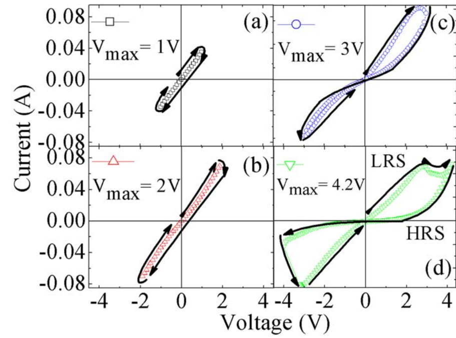

FIG. 2. (Color online) *I-V* curves of Al/STON-*a*/Al for (a) $V_{max}=\pm 1$ V, (b) $V_{max}=\pm 2$ V, (c) $V_{max}=\pm 3$ V, and (d) $V_{max}=\pm 4.2$ V.

In order to achieve resistance R_{total} switching and to determine the threshold voltage, the voltage bias *V* was swept from 0 V → maximum positive voltage in V^+ contact → maximum negative voltage → 0 V, in cycles while the current *I* was measured. The measurements are shown in Figs. 2 and 3 for both samples. For sample STON-*a*, the maximum applied voltages were (a) ±1 V, (b) ±2 V, (c) ±3 V and (d) ±4.2 V for each cycle (see Fig. 2). During the first two cycles between +1 and −1 V and between +2 and −2 V, the system revealed an almost linear behavior. When the voltage was swept between +3 and −3 V, the resistance increased leading to a small hysteresis effect as displayed in Fig. 2(c). A voltage of ±4.2 V was applied to stabilize the switching behavior and to enhance the resistance ratio R_{HRS}/R_{LRS}. By increasing the positive voltage from +3 to +4.2 V, the R_{total} switches from the LRS to the HRS and can be switched reversible (Fig. 2 of supplementary information)[11] by the application of a negative voltage of −4.2 V. It should be noted that the resistance in the HRS can be achieved during the first cycle if the appropriate threshold voltage is applied. This threshold voltage during the electroformation process increases the Al/STON-*a*/Al resistance in an irreversible manner and facilitates resistance switching by sweeping the voltage between −4.2 and 4.2 V.

Four-probe measurements (I^+, V^+, V^-, I^-) were performed before electroformation as well as in HRS and LRS of the (V^+, V^-) MOM in order to measure the R_s resistance and to compare it with the interface resistances $R_{i1}+R_{i2}$. The resistance measured by the four-point probe (R_s) was three orders of magnitude lower than the resistance measured by the two-point probe (R_{total}) and was independently of HRS or

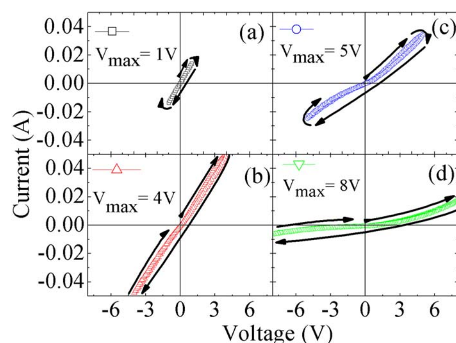

FIG. 3. (Color online) *I-V* curves of Al/STON-*b*/Al for (a) $V_{max}=\pm 1$ V, (b) $V_{max}=\pm 4$ V, (c) $V_{max}=\pm 5$ V, and (d) $V_{max}=\pm 8$ V.

Author complimentary copy. Redistribution subject to AIP license or copyright, see http://apl.aip.org/apl/copyright.jsp

LRS. Indeed, metals with low work functions like indium (4.09 eV) (Ref. 17) and aluminum (4.06 eV), which are frequently used as electric contact materials, forms Schottky barriers.[18] Schottky barrier at the metal-oxide interface (with resistance in the order of $\sim 10-10^2\ \Omega$) is the main contribution to the total resistance of the MOM system. The independency of R_s upon the HRS and LRS changes confirms that switching between the two resistance states takes place at the Al/STON-*a* interfaces and not in the STON-*a* sample (Fig. 3 of supplementary information).[11]

To localize where the switching events appear [i.e., at the anode (V^+) or cathode (V^-)], an additional contact V_a [see Fig. 1(a)] was made. Two *I-V* cycles were measured by the two-point probe method between V^+ and V_a with maximum voltages of ± 1 and ± 4.2V. With the ± 1 V voltage cycle, a linear *I-V* dependency was measured where the Ohmic resistance is equal to LRS (Fig. 4 of supplementary information).[11] This resistance value is higher than for non-electroformed system indicating that a pair of the anode (V^+) and additional cathode (V_a) is already electroformed. The same switching behavior is obtained, as for the previously electroformed Al/STON-*a*/Al, when the two-point measurements are performed with the voltage of ± 4.2 V. This shows that adding the cathode V_a does not alter the state of the (V^+V^-) MOM system, while the *I-V* curve with a maximum of ± 1 V between V_a and cathode V^- shows a nondegraded low resistance. A further increase of the voltage until ± 4.2 V repeats the electroformation procedure observed between V^+ and V^- [see Figs. 2(c) and 2(d)]. These experiments confirm that the high voltage stress induces a symmetry breaking at the anode interface (V^+) of the MOM, leading to stable resistive switching independent of the additional contact position (cathode). This is in agreement with the anode switching detected in other $SrTiO_3$ based materials.[2,19]

Two-point *I-V* curves for Al/STON-*b*/Al were measured between V^+ and V^- and are presented in Fig. 3. The maximum applied voltages were increased stepwise from ± 1 to ± 8 V for each 0 V$\rightarrow$maximum positive voltage in V^+ contact$\rightarrow$maximum negative voltage$\rightarrow$0 V cycle. The *I-V* curves of the system show a linear behavior with the same slope until 4 V. The rectifying behavior was induced by application of threshold voltages ≥ 4 V. A negative voltage as high as -8 V was not enough to switch the resistance of the Al/STON-*b*/Al into LRS, which is twice higher compared to Al/STON-*a*/Al, where the resistance switching was achieved. Similar to Al/STON-*a*/Al, the increasing of the resistance in Al/STON-*b*/Al was assigned to the interfaces.

A model of electroformation and switching in Al/$SrTiO_{3-x}N_y$/Al could be suggested considering mixed ion-electron conductivity concept.[20,21] Before the electroformation, the Al/$SrTiO_{3-x}N_y$/Al stays in LRS and the *I-V* curves at low voltages exhibit Ohmic behavior with the resistance values mostly defined by metal/ceramic interfaces (Fig. 5 of supplementary information).[11] By increasing the positive voltage, both types of samples (with and without stacking faults) switch the resistance into HRS, which can be explained by oxygen/nitrogen ions attraction to the anode interface. Those ions form an interfacial layer, which increases Schottky barrier height of the anode interface and decrease the electron current.[22,23] During the process of ion migration toward the anode, the bulk ceramic $SrTiO_{3-x}N_y$ for both types of samples acts as a source[24] of oxygen/nitrogen, while only samples with characteristic stacking faults behave as a sink of these ions under reverse voltage polarity. Samples without stacking faults exhibit rectifying HRS behavior, which is not changed under high negative voltages confirming the stability of Schottky barrier. An explanation of such stability could be the blocking of the ions at the metal/ceramic interface due to the lack of defects that act as channels for the migration. But the possibility of successful electroformation and reversible switching cannot be excluded for this type of samples applying other methods. For our experimental conditions, taking into account identical electroformation procedure, pads size, etc., the nanostructure defects is the key factor that influences the switching.

In conclusion, we showed that the nanostructure engineering of defects is important for electroformation and resistance switching in Al/$SrTiO_{3-x}N_y$/Al. The reversible and stable resistance switching is facilitated by stacking faults near the surface. Thus we consider a mechanism of the switching as power-driven oxygen/nitrogen reversible migration at the anode interface, where the stacking faults serve as channels for the ionic transport.

The authors thank F. La Mattina, I. Riess and L. Gauckler for fruitful discussions and ETHZ-EMEZ for TEM facilities. The work was supported by Swiss National Science Foundation and by the NCCR MaNEP.

[1] C. Rossel, G. I. Meijer, D. Bremaud, and D. Widmer, J. Appl. Phys. **90**, 2892 (2001).
[2] D. S. Jeong, H. Schroeder, U. Breuer, and R. Waser, J. Appl. Phys. **104**, 123716 (2008).
[3] K. Szot, W. Speier, and W. Eberhardt, Appl. Phys. Lett. **60**, 1190 (1992).
[4] R. Waser and M. Aono, Nature Mater. **6**, 833 (2007).
[5] F. La Mattina, J. G. Bednorz, F. Alvarado, A. Shengelaya, and H. Keller, Appl. Phys. Lett. **93**, 022102 (2008).
[6] X. Li, C. H. Tung, and K. L. Pey, Appl. Phys. Lett. **93**, 072903 (2008).
[7] K. Szot, R. Dittmann, W. Speier, and R. Waser, Phys. Status Solidi (RRL) **1**, R86 (2007).
[8] A. Shkabko, M. H. Aguirre, A. Weidenkaff, I. Marozau, and T. Lippert (unpublished).
[9] A. Shkabko, M. H. Aguirre, I. Marozau, M. Dobeli, T. Lippert, M. Mallepell, and A. Weidenkaff, Mater. Chem. Phys. **115**, 86 (2009).
[10] D. K. Schroder, *Semiconductor Material and Device Characterization* (Wiley, Hoboken, 2006).
[11] See EPAPS Document No. E-APPLAB-94-091920 for the supplementary figures. For more information on EPAPS, see http://www.aip.org/pubservs/epaps.html.
[12] K. J. Kim, D. W. Moon, S. H. Nam, W. J. Lee, and H. G. Kim, Surf. Interface Anal. **23**, 851 (1995).
[13] I. L. Strydom and S. Hofmann, J. Electron Spectrosc. Relat. Phenom. **56**, 85 (1991).
[14] R. P. Vasquez, J. Electron Spectrosc. Relat. Phenom. **56**, 217 (1991).
[15] Y. Haruyama, Y. Aiura, H. Bando, Y. Nishihara, and H. Kato, J. Electron Spectrosc. Relat. Phenom. **88**, 695 (1998).
[16] P. A. W. van der Heide, Q. D. Jiang, Y. S. Kim, and J. W. Rabalais, Surf. Sci. **473**, 59 (2001).
[17] O. N. Tufte and P. W. Chapman, Phys. Rev. **155**, 796 (1967).
[18] J. Robertson and C. W. Chen, Appl. Phys. Lett. **74**, 1168 (1999).
[19] S. F. Karg, G. I. Meijer, J. G. Bednorz, C. T. Rettner, A. G. Schrott, E. A. Joseph, C. H. Lam, M. Janousch, U. Staub, F. La Mattina, S. F. Alvarado, D. Widmer, R. Stutz, U. Drechsler, and D. Caimi, IBM J. Res. Dev. **52**, 481 (2008).
[20] I. Riess, J. Electroceram. **17**, 247 (2006).
[21] K. Szot, W. Speier, G. Bihlmayer, and R. Waser, Nature Mater. **5**, 312 (2006).
[22] J. J. Yang, M. D. Pickett, X. M. Li, D. A. A. Ohlberg, D. R. Stewart, and R. S. Williams, Nat. Nanotechnol. **3**, 429 (2008).
[23] A. Sawa, T. Fujii, M. Kawasaki, and Y. Tokura, Appl. Phys. Lett. **85**, 4073 (2004).
[24] R. Muenstermann, R. Dittmann, K. Szot, S. B. Mi, C. L. Jia, P. Meuffels, and R. Waser, Appl. Phys. Lett. **93**, 023110 (2008).

Author complimentary copy. Redistribution subject to AIP license or copyright, see http://apl.aip.org/apl/copyright.jsp